Applied Catalysis B: Environmental 176–177 (2015) 347–353

Contents lists available at ScienceDirect

Applied Catalysis B: Environmental

journal homepage: www.elsevier.com/locate/apcatb

Preparation of porous metal-ion-doped titanium dioxide and the photocatalytic degradation of 4-chlorophenol under visible light irradiation

Naoto Nishiyama [a], Yuhei Fujiwara [a], Kenta Adachi [a], Kei Inumaru [b], Suzuko Yamazaki [a,*]

[a] Division of Environmental Science and Engineering, Graduate School of Science and Engineering, Yamaguchi University, Yamaguchi 753-8512, Japan
[b] Department of Applied Chemistry, Faculty of Engineering, Hiroshima University, Higashi-Hiroshima 739-8527, Japan

ARTICLE INFO

Article history:
Received 23 February 2015
Received in revised form 6 April 2015
Accepted 8 April 2015
Available online 11 April 2015

Keywords:
Visible-light responsive photocatalyst
Metal ion doped TiO_2
Chromium ion doped TiO_2
4-Chlorophenol
Sol–gel method

ABSTRACT

Aiming at developing a highly active photocatalyst to decompose organic compounds under visible light irradiation, we have prepared metal ion doped TiO_2 (M-TiO_2) by conducting dialysis in sol–gel method. Dialysis leads to the formation of mesoporous materials with surface area larger than 200 $m^2 g^{-1}$ but the metal ions should be added into the TiO_2 sol at pH 3 in order to avoid their losses during dialysis. Among seven metal ions tested as dopants, Pt-TiO_2 and Cr-TiO_2 showed higher photocatalytic activity for the degradation of 4-chlorophenol under visible light irradiation. The photocatalytic activity of Cr-TiO_2 was strongly affected by the doping amount of Cr ion and the optimal value was evaluated to be 0.68–1.30 atom%. X-ray photoelectron spectroscopy analyses showed the Cr ion was present mainly in Cr(III). The Cr-TiO_2 can be used safely for a practical application to remediate environmental contamination instead of expensive Pt-TiO_2.

1. Introduction

Titanium dioxide has been widely studied as a photocatalyst for applications to environmental remediation since it is stable, harmless and inexpensive and has a high reactivity for decomposition of harmful compounds [1–6]. However, TiO_2 is active only under ultraviolet (UV) irradiation ($\lambda < 388$ nm) due to its large band gap energy of 3.0–3.2 eV, resulting in a low efficiency to utilize solar radiation. Many attempts have been devoted to extend the spectral response of TiO_2 to visible light [7]. Doping of transition metal ion is one of the most reported approaches and believed to achieve the band gap narrowing by forming impurity energy levels in the TiO_2 band gap [8–14]. Doping has been attempted physically by metal ion implantation and vapor deposition or chemically by co-precipitation and sol–gel method. Anpo and co-workers demonstrated Cr or V ions implanted TiO_2 is active under visible light irradiation ($\lambda > 450$ nm) and the ions are present in a highly dispersed and isolated state in octahedral coordination, suggesting that the ions are incorporated into the lattice positions of the TiO_2 in place of the Ti ions [15,16]. They also described that the photocatalytic reaction did not proceed on the chemically doped TiO_2 under visible light irradiation ($\lambda > 450$ nm), in which the metal ions were present as oxide aggregates. Although metal ion implantation is able to result in atomic level doping, it requires expensive equipment. Shen et al. achieved vanadium doping of TiO_2 at the atomic level by a new facile liquid phase atomic layer deposition method to improve the photocatalytic activity under visible light [17]. On the other hand, by using a simple sol–gel method, Kim et al. synthesized Pt ion doped TiO_2 and demonstrated its visible light photocatalytic activities for the oxidative and reductive degradation of chlorinated organic compounds [18]. Choi et al. adopted the similar sol–gel method to synthesize TiO_2 doped with 13 different metal ions and compared the effects of individual dopants on the resulting physicochemical properties [19]. They mentioned that Pt- and Cr-doped TiO_2, which had relatively high percentage of rutile, showed significantly enhanced visible light photocatalytic activity, suggesting that the presence of the rutile structure in the doped TiO_2 may affect photocatalytic activities. Wang et al. prepared indium-doped TiO_2 by the sol–gel method and showed improved photocatalytic activity due to the existence of a unique chemical species, O–In–Cl_x on the surface under visible light irradiation [20].

Specific surface area of photocatalysts is one of the important factors for improving the activity in heterogeneous photocatalytic decomposition of organic compounds. A large number of efforts has been made to prepare mesoporous TiO_2 with high surface area and uniform pore size [21]. Xu and Anderson reported that

* Corresponding author. Tel.: +81 83 933 5763; fax: +81 83 933 5763.
E-mail address: yamazaki@yamaguchiu.ac.jp (S. Yamazaki).

http://dx.doi.org/10.1016/j.apcatb.2015.04.015
0926-3373/

specific surface area and porosity of TiO_2 xerogel prepared by sol–gel method increased with an increase in pH of the sol by dialysis [22]. Most metal oxide particles are charged at low pH and thus, they repel each other upon approach, forming a stable colloidal suspension. However, when the pH is increased by gradually removing protons from the suspension through dialysis, the particles tend to undergo aggregation, leading to the formation of large pores. We synthesized porous Pt-TiO_2 with pores of ca. 4 nm in diameter and BET surface area higher than 200 $m^2\,g^{-1}$ by using only water as the solvent and conducting dialysis in the sol–gel method and demonstrated to have superior photocatalytic activity for the photodegradation of 4-chlorophenol (4-CP) under both ultraviolet and VL irradiation [23]. However, platinum is highly expensive and the use of less expensive metal ions is more favorable. In this study, we prepared porous TiO_2 doped with various metal ions by using our synthetic method having dialysis procedures and examined the photocatalytic activity for the degradation of 4-CP in aqueous solutions under visible light irradiation.

2. Experimental

2.1. Preparation and characterization of M-TiO_2

Method A, as shown in Scheme 1 indicates the synthetic method for porous M-TiO_2 photocatalysts which is the same sol–gel method as in our previous paper for Pt-TiO_2 [23]. As the metal ion precursors, $H_2PtCl_6{\cdot}6H_2O$, $CrCl_3{\cdot}6H_2O$, $CuCl_2$, $CoCl_2{\cdot}6H_2O$, $FeCl_3{\cdot}6H_2O$, K_2RuCl_6 or $RuCl_3{\cdot}nH_2O$ were used. After peptization in an aqueous solution at pH ≤ 1 for 6 days, the highly dispersed TiO_2 sol containing the metal ions was dialyzed in 2750 ml of water using a molecularly porous dialysis tube (molecular weight cut-off: 3500) for 3 days

until approximately pH 4 was obtained. The water was exchanged once a day and the concentration of the metal ions removed out of the TiO_2 sol through the dialysis tube was determined by inductively coupled plasma spectroscopy (Varian, ICP-AES Liberty Series II). Then, the sol was dried in an oven at 40 °C for 3 days and the resulting gel was sintered at 100–500 °C (ramping rate at 3 °C min^{-1} and keeping the desired temperature for 2 h). The obtained xerogel was crushed into powders by using mortar and pestle. In this paper, the contents of metal ions in the samples are denoted as the nominal atomic percentage (atom%) against all metal ions (M and Ti). The value of atom% was calculated on the basis of the ICP-AES measurement which determined the concentration of M^{n+} removed from the TiO_2 sol. Undoped TiO_2 powder was prepared according to the above procedures without the metal ion precursors.

Crystal structure of the M-TiO_2 was examined by X-ray diffraction (XRD, Rikagaku RINT-2500) analysis with Cu Kα radiation (40 kV, 100 mA) at 2θ angles from 10° to 90° with a scan speed of 4° min^{-1}. The Brunauer–Emmett–Teller (BET) surface area was measured with nitrogen as the adsorptive gas by automatic surface area analyzer (Shimadzu, Trister II 3020). Diffuse reflectance UV–vis spectra of the M-TiO_2 were obtained using a spectrophotometer (Nippon Bunko, V-670). X-ray photoelectron spectroscopy (XPS) analysis was carried out through KRATOS ESCA-3400 system. The Cr-TiO_2 powder was compressed into a pellet for the XPS measurements. The number of data accumulation was 120 for Cr 2p and 10 for other elements.

2.2. Determination of photocatalytic activity

Photocatalytic activity was evaluated at 30 °C by the degradation of 4-CP in aqueous solutions suspended with M-TiO_2 powders. After air was purged through the suspension for 30 min under vigorously stirring, a 150 W halogen lamp was ignited. The light intensity through a long pass filter (Edmund, cut-on wavelength: 400 nm) was measured to be 63 mW cm^{-2} (Koito, Memory Sensor MES-101 with IKS-37). Aliquots of the suspension were withdrawn at appropriate times and centrifuged at 2000 rpm for 15 min. The supernatant liquid was filtrated through a 0.45 μm filter and then analyzed by a high performance liquid chromatograph (HPLC, Shimadzu) equipped with a UV–vis detector and a C18 column (Shim-pack, VP-ODS 4.6 mm × 25 cm).

3. Results and discussion

3.1. Loss of metal ions during dialysis

Fig. 1 indicates the absorption spectra of the TiO_2 sol and M-TiO_2 sol (M = Pt, Cr, Fe, Ru(IV), and Ru(III)) just before the dialysis. The broken lines in Fig. 1 show the values calculated by adding the spectra of the TiO_2 sol to those of an aqueous solution containing each metal ion at pH 1. All absorption spectra of the M-TiO_2 sol

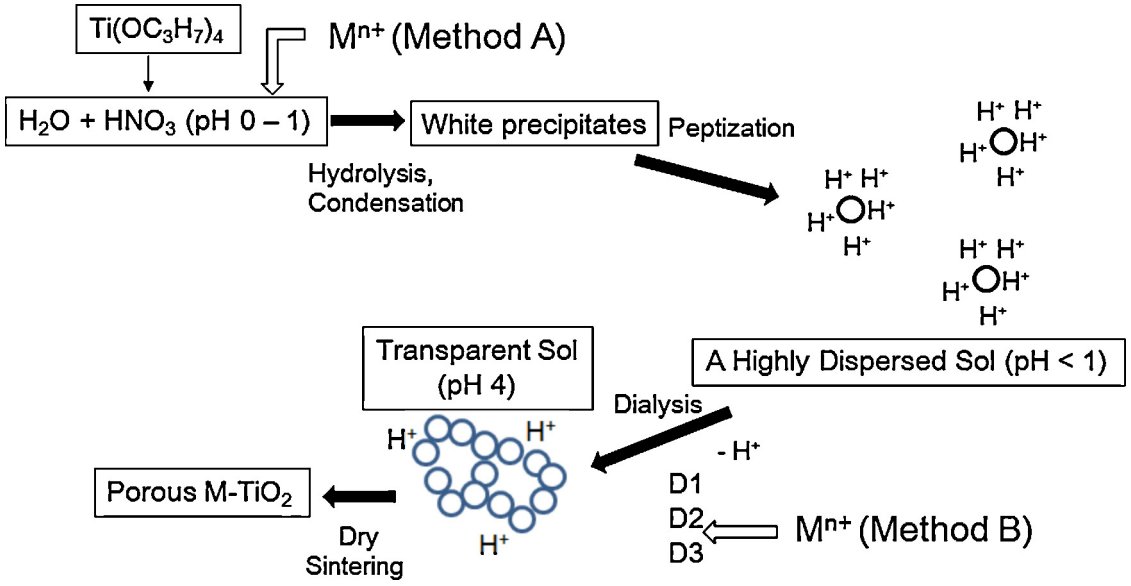

Scheme 1. Synthetic method for porous M-TiO_2 photocatalysts.

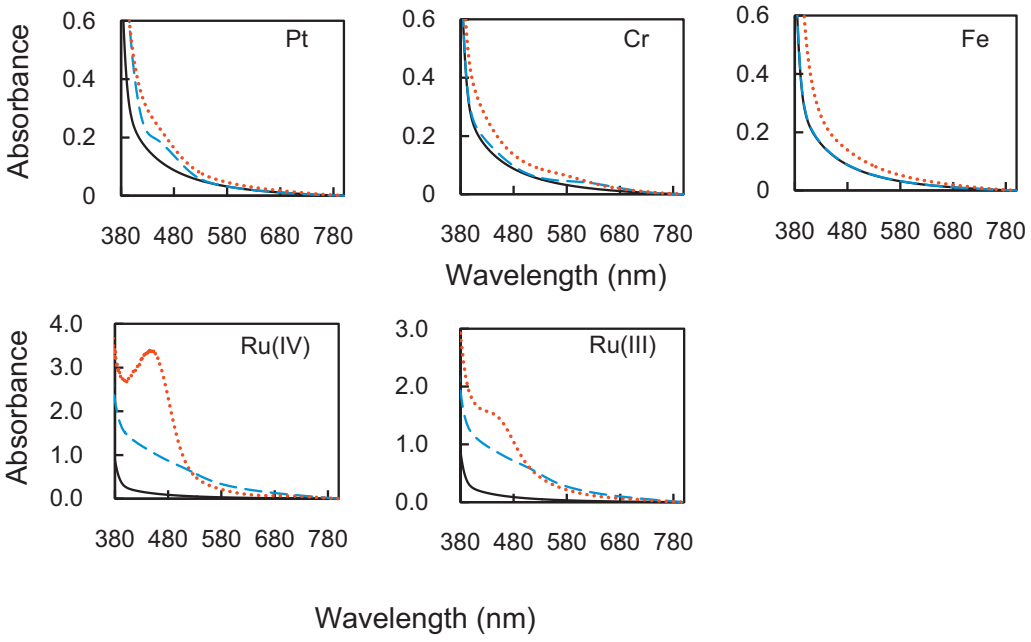

Fig. 1. Absorption spectra of TiO_2 sol (—) and M-TiO_2 sol (·····) before dialysis. The broken line indicated the absorption spectra calculated with sum of those for TiO_2 sol and aqueous metal-ion solutions.

were higher than those of the calculated spectra. Such an increase in the absorption might be due to the charge-transfer transition of electrons between the *d*-orbital of the metal ion and the conduction band or the valence band of TiO_2. Especially, the absorption spectra of the Ru(IV)-TiO_2 or Ru(III)-TiO_2 sol showed an intense peak at ca. 440 nm, which was not present in the spectrum of Ru(IV) or Ru(III) ion in water, indicating that a strong interaction between the TiO_2 particles and Ru(IV) or Ru(III) ion. Choi et al. also described that the addition of Ru(III) in TiO_2 colloids gave a strong absorption band at 437 nm, which was ascribed to the incorporation of Ru(III) ions in the TiO_2 lattice [24].

Some metal ions were removed from the M-TiO_2 sol during the dialysis. Fig. 2 indicates that Pt(IV) ion hardly lost whereas more than 90% of Co(II) or Cu(II) was lost even in the first dialysis (D1). In the case of Cr(III) or Fe(III), 57.7 or 53.9% in D1, 1.21 or 5.13% in the second dialysis (D2) were lost. It is noted that the loss in D2 remarkable decreased than that in D1 and no loss was observed in the third dialysis (D3) for all metal ions tested. This fact suggests the loss of metal ions depends on the pH since the pH of the M-TiO_2 sol increased from pH ≤ 1 to pH 2–4 after D1–D3, respectively. Table 1 lists the total loss from D1 to D3 in the column denoted as method A. In an aqueous solution, oxide particles have hydrated surface which is dominated by OH surface group. The surface has positive or negative charges, depending on pH in the solution. At

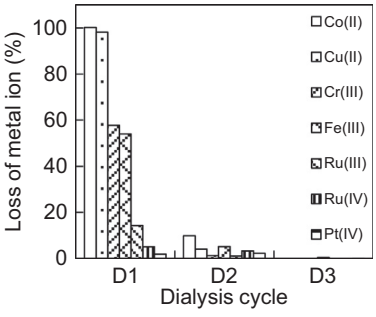

Fig. 2. Loss of metal ions during dialysis.

Table 1
Total loss of metal ions during three dialysis operations.

Metal ion	Loss during dialysis (%)	
	Method A	Method B
Pt(IV)	4.1	
Ru(IV)	8.2	
Ru(III)	15.3	
Cr(III)	59.0	0.45
Fe(III)	59.5	0
Cu(II)	100	71.9
Co(II)	100	90.6

pH ≤ 1 after peptization for 6 days, the TiO_2 particles are charged positively since the isoelectric point of TiO_2 is ca. 6.0.

$$-MOH + H^+ \rightleftharpoons -MOH_2^+ \quad (1)$$

Since Pt(IV) was added as $H_2PtCl_6{\cdot}6H_2O$, it exists as $[PtCl_6]^{2-}$ which can interact with the positively charged TiO_2 particles. As shown in Fig. 1, Ru(III) and Ru(IV) have strong interaction with TiO_2 causing the intense absorption peak in visible region. Such interactions with TiO_2 might be responsible for the lower loss of these three ions during the dialysis. On the other hand, other metal ions exists as $[M(H_2O)_6]^{n+}$ which enhances the loss due to an electrostatic repulsion with the positively charged TiO_2. As the pH increases to pH 2 by conducting D1, the surface positive charge on TiO_2 particles decreases. Besides, some of $[Cr(H_2O)_6]^{3+}$ and $[Fe(H_2O)_6]^{3+}$ are hydrolyzed to $[Cr(H_2O)_5(OH)]^{2+}$ and $[Fe(H_2O)_5(OH)]^{2+}$, since pK_h values (K_h: hydrolysis constant for the equation of $[[M(OH)]^{2+}][H^+]/[M^{3+}]$) are 4.0 and 2.8, respectively [25,26]. The formation of hydroxo complex reduces the positive charge on the metal ion and it is well known that hydroxo complex can easily interact with surface OH on oxides particles. As a result, ca. 42–46% of Cr(III) or Fe(III) remained in the TiO_2 sol after D1. On the other hand, pK_h values for Cu(II) and Co(II) are 7.9 and 10.5, respectively [27,25] and no hydrolysis occurs at pH 2, resulting in the loss more than 90% in D1. As the pH increases by repeating dialysis, the surface positive charge on the TiO_2 particles decreases and more metal ions are hydrolyzed to hydroxo complex, leading to the reduction in the electrostatic repulsion. We changed the time

to add the metal ion precursors from the initial step at pH ≤ 1 to the highly dispersed sol at pH 3 obtained just after D2 (hereafter, denoted as method B). As expected, we found that by method B, the loss of Cr(III) or Fe(III) after D3 was completely suppressed and 28.1% of Cu(II) or 9.4% of Co(II) was doped as shown in Table 1. It should be noted that most of Cl^- ion contained in the metal ion precursors were removed during dialysis, suggesting that $[PtCl_6]^{2-}$ and $[RuCl_6]^{2-}$ were hydrolyzed [28].

3.2. Characterization and photoactivities of M-TiO_2

Table 2 lists the properties of the M-TiO_2 which was synthesized with an addition of 0.5 atom% metal ion by method A and was sintered at 200 °C. Since ca. 60% of Cr(III) or Fe(III) was lost during the dialysis as described above, the amount of Cr(III) or Fe(III) incorporated in TiO_2 was estimated to be 0.2 atom%. The XRD patterns of all M-TiO_2 consisted of broad peaks attributable to anatase and the crystalline size was estimated to be 4.3–5.0 nm from the anatase (1 0 1) phase by using Scherrer equation. No diffraction peaks attributable to the metal ions were observed, suggesting that the metal ions were dispersed within TiO_2 and did not form the separate impurity phases. Band gap energy was evaluated from Tauc plots, suggesting that the doping of the metal ions in TiO_2 lowered it by 0.12–0.28 eV. The BET surface area was slightly increased by doping. On the other hand, the adsorption and desorption isotherms of all M-TiO_2 samples coincided with TiO_2, showing hysteresis which clearly indicated capillary condensation transition. As a result, the Barrett–Joyner–Halenda (BJH) method accounting for capillary condensation in the pores showed that all M-TiO_2 samples have pores of ca. 3.7 nm, as the same as TiO_2.

The photocatalytic activity of M-TiO_2 was examined by the degradation of 4-CP under visible light. In the investigation aimed at the remediation of wastewater, 4-CP has been often selected as a model compound because of its highly toxicity and poorly degradable property. We reported in our previous paper [23] that 4-CP was completely degraded on 0.5 atom% Pt-TiO_2 at the visible light irradiation of 150 min and then the degradation of byproducts such as *p*-benzoquinone and hydroquinone was enhanced. We confirmed that 90.7% of 4-CP was completely mineralized at the irradiation of 390 min by using total organic carbon analyzer. In this paper, we employ the conversion of 4-CP for comparing the photocatalytic activity of M-TiO_2 prepared under various conditions. Fig. 3 shows the photocatalytic activity of the samples listed in Table 2. It is well-known that 4-CP is degraded on TiO_2 under visible light because of the formation of surface complex between TiO_2 and phenol moiety of 4-CP [29]. The photocatalytic activity higher than TiO_2 was observed only for Pt-TiO_2 and Cr-TiO_2. Deactivation of TiO_2 occurred as the following order: Ru(III)-TiO_2, Ru(IV)-TiO_2 > Fe-TiO_2. As shown in their band-gap

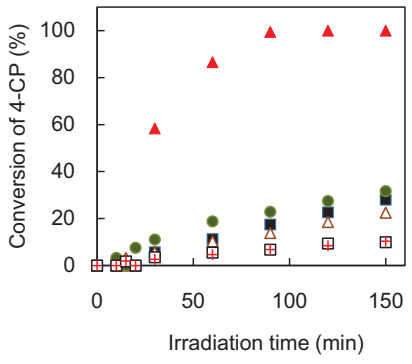

Fig. 3. Time course of the 4-CP conversion of TiO_2 (■), Pt- (▲), Cr- (●), Fe- (△), Ru(IV)- (□), and Ru(III)-TiO_2 (+).

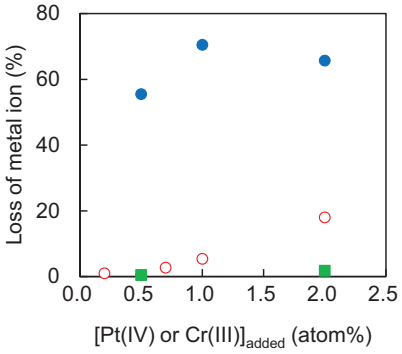

Fig. 4. Loss of Pt ion (method A: ■) and Cr ion (method A: ●, method B: ○) during dialysis.

energy, these samples absorb the visible light more efficiently than Pt-TiO_2 and Cr-TiO_2. Thus, the doped Ru(III), Ru(IV), and Fe(III) act as the recombination centers of the photogenerated holes and electrons. Choi et al. reported that Fe-TiO_2 showed a slightly increased photocatalytic activity while Ru(III)-TiO_2 had negligible effect for the degradation of methylene blue when compared to TiO_2 [19]. Zhu et al. also described that Fe-TiO_2 had an increased visible light response for the degradation of methylene blue [30]. These conflicting results with ours can be ascribed to the structural modification related to iron incorporation. Santos et al. described the controversial results observed in literature for the performance of Fe-TiO_2 photocatalyst can be attributable to the findings that the presence of segregated hematite in Fe-TiO_2 grain boundaries can affect the separation of photogenerated charges (electron and hole pairs) [31]. Zhu et al. prepared Fe-TiO_2 by combining sol–gel method with hydrothermal treatment and described that the degressive content of Fe^{3+} dopant from the surface to the interior of TiO_2 may result in the high photocatalytic activity [32]. Hereafter, we focus on the increase in the photocatalytic activity of Cr-TiO_2 because platinum is extremely rare and expensive.

3.3. Optimal condition to synthesize active Cr-TiO_2

Fig. 4 indicates the effect of the added amount of Cr(III) or Pt(IV) on the loss during the dialysis. When 0.5, 1.0, 2.0, and 5.0 atom% Cr(III) were added by method A, the loss of Cr(III) ion was estimated to be 55.5, 70.5, 65.7 and 49.0%, respectively. As a result, 0.22, 0.30, 0.69, and 2.55 atom% Cr(III) was doped within TiO_2. By using method B, the loss of Cr(III) was hardly observed with the addition less than 0.5 atom% and increased from 2.71% to 18.0% when the

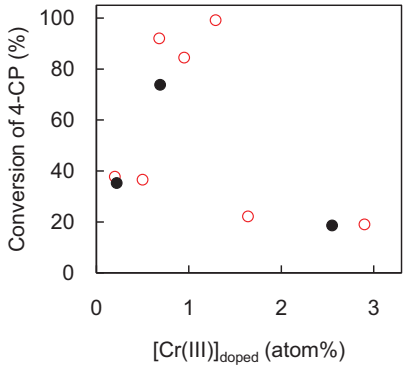

Fig. 5. Effect of the doping amount of Cr ion on the conversion of 4-CP at the irradiation of 150 min. The Cr-TiO_2 was prepared by method A (●) or method B (○).

Table 2
Crystalline size, band gap energy, BET surface area and doping amount of metal ions when M-TiO_2 was synthesized with an addition of 0.5 atom% metal ion by method A.

	Crystalline size (nm)	Band gap (eV)	BET surface area ($m^2\ g^{-1}$)	Amount of metal ion (atom%)
TiO_2	4.3	3.06	237	–
Pt(IV)-TiO_2	4.3	2.90	263	0.5
Cr(III)-TiO_2	5.0	2.94	245	0.2
Fe(III)-TiO_2	4.3	2.87	263	0.2
Ru(IV)-TiO_2	4.6	2.78	274	0.5
Ru(III)-TiO_2	4.5	2.80	255	0.4

Table 3
Effect of doping amount of Cr ion on BET surface area and band gap energy of Cr-TiO_2.

$[Cr(III)]_{doped}$ (atom%)	BET surface area ($m^2\ g^{-1}$)	Band gap (eV)
0.198	245	2.95
0.681	253	2.90
0.946	241	2.70
1.64	220	2.79
2.87	213	2.67
6.59	242	2.60

amount of Cr(III) increased from 0.7 to 2.0 atom%. It is worthy to note that in the case of Pt(IV), it hardly lost even at 2.0 atom% by method A. Fig. 5 shows the photocatalytic activity of Cr-TiO_2 which was prepared by both methods and sintered at 200 °C. The optimal doping amount of Cr(III) is estimated to be 0.68–1.30 atom%. Comparison of the activity at the same doping amount indicates that no significant difference is obtained in both methods. Thus, we can conclude that method B is more advantageous because of the suppression of the loss of Cr(III) during the dialysis. Table 3 lists the BET surface area and band gap energy of Cr-TiO_2 prepared by method B. The increase in the doping amount from 0.2 to 6.6 atom% decreases the band gap energy from 2.95 to 2.60 eV. This change in the band gap indicates that the doping of Cr ion lowers the conduction band edge. Such a shift in the conduction band edge was described for Pt-TiO_2 [18,23]. This means that higher doping amount of Cr ion is better to absorb visible light. However, Fig. 5 shows that the doping higher than 1.3 atom% decreases the photocatalytic activity. This finding will be discussed later. Fig. 6 indicates the XRD patterns of 0.82 atom% Cr-TiO_2 sintered at 100–500 °C. Higher sintering temperature enhances the crystallization of anatase, the transformation to rutile occurs at 400 °C and rutile and anatase coexist at 500 °C. The BET surface area decreases as an increase in sintering temperature: 308, 261, 191, 133 and 59 $m^2\ g^{-1}$ at 100, 200, 300, 400 and 500 °C, respectively. Fig. 7 shows that the photocatalytic activity of Cr-TiO_2 sintered at 200 °C is the best and decreased by the following order: 200 °C > 300 °C ≈ 400 °C > 500 °C > 100 °C. This can be explained by the fact that anatase crystallite with larger surface area has higher activity to decompose organic compounds [33]. Although the specific surface area was the largest for Cr-TiO_2 sintered at 100 °C, the crystalline size of anatase estimated by Scherrer equation is the smallest, suggesting the presence of more amorphous phase.

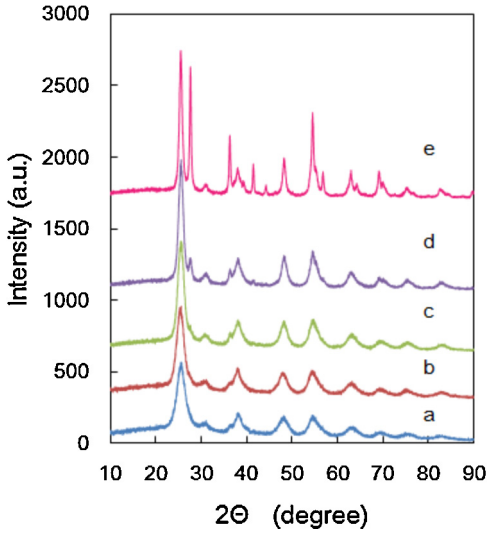

Fig. 6. XRD patterns of 0.82 atom% Cr-TiO_2 prepared by method B and calcined at (a) 100, (b) 200, (c) 300, (d) 400 and (e) 500 °C.

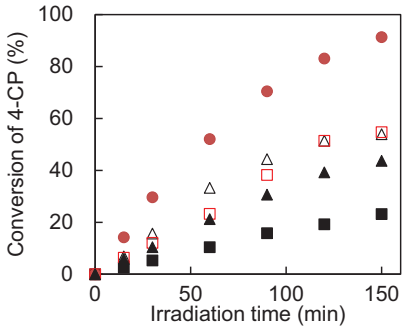

Fig. 7. Effect of sintering temperature on the conversion of 4-CP on 0.82 atom% Cr-TiO_2. 100 (■), 200 (●), 300 (△), 400 (□) and 500 °C (▲).

In order to understand that the doping of Cr ion higher than 1.3 atom% decreases the photocatalytic activity, we compared the photocatalytic activity of Pt-TiO_2 synthesized by methods A and B. Fig. 8 shows that the photocatalytic activity is not dependent on the preparation method similarly as Cr-TiO_2. However, no decrease in photocatalytic activity is observed even at 2.0 atom% Pt-TiO_2, although 2.0 atom% Cr-TiO_2 has much lower activity than 0.68–1.30 atom% Cr-TiO_2. Shen et al. described that the atomic level doping of transition metal was important to get photocatalytic activity under visible light [17]. The formation of the dopant oxide aggregates created electron–hole recombination centers decreasing the catalytic activity even though visible light absorption was increased. Wang et al. mentioned that the photocatalytic activity of TiO_2 doped with indium decreased at the higher content

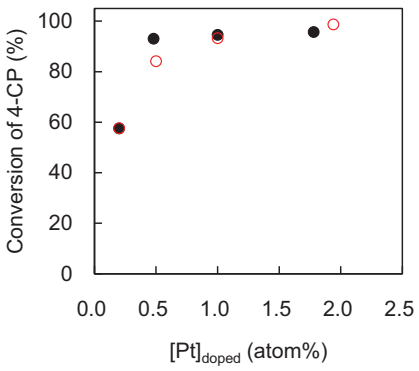

Fig. 8. Effect of the doping amount of Pt ion on the conversion of 4-CP at the irradiation of 90 min. The Pt-TiO_2 was prepared by method A (●) or method B (○).

than 10 mol% because of the formation of In_2O_3 whose characteristic diffractive peak was detected in the XRD patterns [20]. In our Cr-TiO_2, no diffraction peak of Cr_2O_3 was detected even with 6.6 atom% Cr-TiO_2. Thus, it is ruled out that the formation of Cr_2O_3 causes the deactivation of Cr-TiO_2. For any photocatalytic reaction, the lifetimes of photogenerated electrons and holes must be long enough to allow them reach the surface of the photocatalyst. In the TiO_2 photocatalysis under UV illumination, it is well-known that by incorporation of transition metal ions, new trapping sites are introduced which affect the photocatalytic activity, depending on the lifetime of the charge carriers [34]. Choi et al. reported that metal ion dopants should act as both electron traps and hole traps to be photoactive [24]. Trapping either an electron or a hole alone is ineffective because the immobilized charge species quickly recombines with its mobile counterparts. By doping Mo^{5+} in TiO_2, ESR studies have shown that Mo^{5+} and Mo^{6+} coexisted in the TiO_2 lattice where they acted as a hole trap and an electron trap, respectively. As a result, Mo-TiO_2 showed high photocatalytic activity. They also described that photoexcited electron in TiO_2 doped with Cr^{3+} which can serve only as hole traps quickly recombines with a trapped hole in Cr^{3+} (Cr^{4+}). Thus, we tried to measure the valence state of the metal ions in Cr-TiO_2 and Pt-TiO_2. Fig. 9 shows the XPS spectra of 1.3 atom% and 6.6 atom% Cr-TiO_2. Binding energy was corrected with characteristic peak of carbon $1s_{1/2}$ as 284.5 eV. The peak at 577.5 eV observed with 1.3 atom% and 6.6 atom%

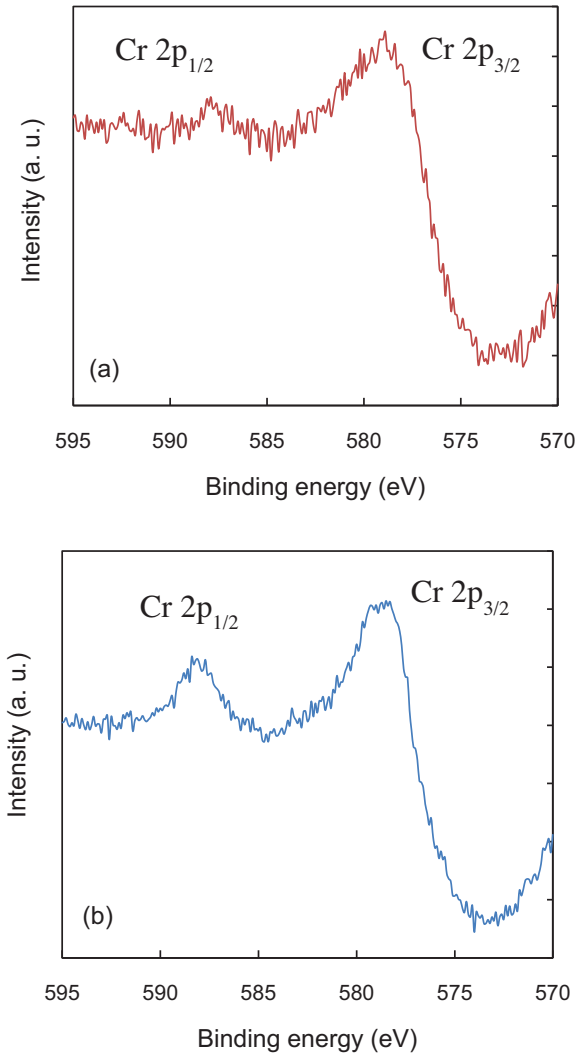

Fig. 9. XPS spectra of Cr-TiO_2 of (a) 1.3 atom% and (b) 6.6 atom%.

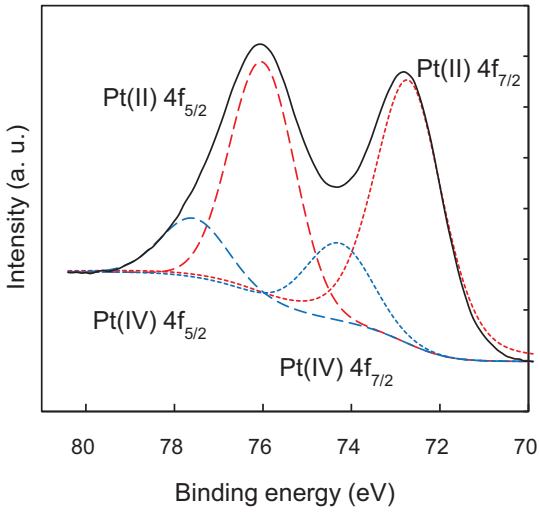

Fig. 10. XPS spectra of 0.5 atom% Pt-TiO_2.

Cr-TiO_2 corresponds to Cr $2p_{3/2}$, indicating clearly the presence of Cr(III) in the sample [35]. Comparison of these spectra reveals that the peaks observed with 1.3 atom% Cr-TiO_2 are broader than those with 6.6 atom% Cr-TiO_2. This might suggest the presence of other valences except for trivalent in 1.3 atom% Cr-TiO_2. Fig. 10 shows XPS spectra of Pt-TiO_2, where the deconvolution of Pt 4f band indicates the presence of Pt(II) and Pt(IV) states. According to the research conducted by Kim et al. on visible light active Pt-TiO_2, the photogenerated electron is trapped by Pt^{4+}, whereas hole is trapped by Pt^{2+} [18]. Some trapped charges may recombine to regenerate the initial redox states. As a result, photogenerated carriers migrate to the surface and subsequently, hole oxidizes 4-CP and electron reacts with oxygen.

$$Pt^{4+} + h\nu \rightarrow Pt^{3+}(\text{or trapped electron}) + h_{VB}{}^{+} \quad (2)$$

$$Pt^{2+} + h\nu \rightarrow Pt^{3+}(\text{or trapped hole}) + e_{CB}{}^{-} \quad (3)$$

$$Pt^{3+} + Pt^{3+} \rightarrow Pt^{2+} + Pt^{4+} \quad (4)$$

In 6.6 atom% Cr-TiO_2, photogenerated electron quickly recombines with a trapped hole (Cr^{4+}).

$$Cr^{3+} + h\nu \rightarrow Cr^{4+}(\text{or trapped hole}) + e_{CB}{}^{-} \quad (5)$$

$$Cr^{4+}(\text{or trapped hole}) + e_{CB}{}^{-} \rightarrow Cr^{3+} \quad (6)$$

Zhu et al. also mentioned that TiO_2 doped with Cr^{3+} had an optimal doping concentration for the degradation of an azoic dye, and the Cr^{3+} concentration in the bulk should not be too high in order to reduce the possibility of over-trapping of photogenerated holes by Cr^{3+} [36]. Although the reason why 1.3 atom% Cr-TiO_2 has much higher activity than 6.6 atom% Cr-TiO_2 remains unclear, the existence of other valence state in 1.3 atom% Cr-TiO_2 might prolong the lifetime of the photogenerated carriers as mentioned in Pt-TiO_2. Hexavalent chromium ion has been considered to be one of the most common pollutants in aquatic environment [37]. The prepared Cr-TiO_2 was tested by boiling water extraction procedure in accordance with International Electrotechnical Commission (IEC) 62321 and the filtrate was analyzed by ICP-AES but no Cr(VI) was detected. Therefore, even if other chromium species except for Cr(III) were present in Cr-TiO_2, we have ascertained that Cr-TiO_2 photocatalyst can be safely used for a practical application to purify wastewater.

Fig. 11 shows the comparison of photocatalytic activity of 1.3 atom% Cr-TiO_2 with Pt-TiO_2, indicating that 1.3 atom% Cr-TiO_2 is more active than 0.2 atom% Pt-TiO_2 and less active than 0.5 atom% Pt-TiO_2. Platinum is very expensive and an extremely scarce in

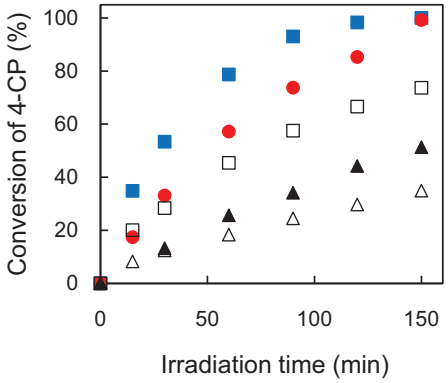

Fig. 11. Comparison of photocatalytic activity of 1.3 atom% Cr-TiO_2 (●), 0.2 atom% Pt-TiO_2 (□) or 0.5 atom% Pt-TiO_2 (■) which was prepared by our method. Data obtained on 0.5 atom% Pt-TiO_2 prepared according to the literature using ethanol as solvent with (▲) and without (△) dialysis were also plotted.

spite of a crucial resource in industries for controlling automobile emissions and developing fuel-cells [38]. Therefore, 1.3 atom% Cr-TiO_2 has more benefit than Pt-TiO_2. The photocatalytic activity of Pt-TiO_2 prepared by hydrolyzing $Ti(OC_3H_7)_4$ in the presence of ethanol was also plotted in Fig. 11. The M-TiO_2 has been often prepared by hydrolyzing titanium alkoxides in an aqueous solution containing ethanol and metal ion precursors [18,20,39,40]. In general, alcohol is served to slow down the hydrolysis reaction of $Ti(OC_3H_7)_4$. Indeed, in the presence of ethanol, hydrolysis and condensation occur in homogeneous solution whereas in our method without ethanol, a white precipitate is formed and dispersed homogeneously by vigorously stirring for a few days. Higher activity of Pt-TiO_2 and Cr-TiO_2 prepared in this study is attributable to higher specific surface area brought by conducing dialysis. However, by introducing dialysis in the presence of ethanol, the BET surface area increased from 131 to 310 $m^2 g^{-1}$ but the photocatalytic activity increased only a little. This suggests the presence of ethanol might affect the growth of TiO_2 nanoparticles although effect of alcohols on the morphology and microstructure is still argument [41–43]. Fig. 11 indicates that higher photocatalytic activity due to higher specific surface area by conducting dialysis is obtained by using only water as the solvent in sol–gel synthesis.

4. Conclusion

In the sol–gel synthesis of TiO_2 photocatalysts, calcination at high temperature is needed to decompose byproducts such as isopropanol from $Ti(OC_3H_7)_4$. However, calcination at high temperature decreases the specific surface area of the photocatalysts and converts anatase phase to less photoactive rutile. By conducting dialysis, the colloid solutions are purified and large pores are formed by gradually removing protons from the surface of the colloid particles. As a result, anatase TiO_2 with high specific surface area can be obtained. We applied this method to synthesize porous M-TiO_2 and found that some metal ions were lost during dialysis, which seems to be related to their hydrolysis constants. In order to avoid the loss, the metal ion should be added into the TiO_2 sol at pH 3 obtained during dialysis, although the photocatalytic activity of M-TiO_2 is not affected by the time of adding when being compared at the same doping amount. We have successfully prepared porous Cr-TiO_2 with the BET surface area higher than 200 $m^2 g^{-1}$ by sintering at relatively low temperature as 200 °C and demonstrated the superior photocatalytic activity under visible light irradiation, which is comparable to that of Pt-TiO_2.

Acknowledgments

This work was partially supported by Japan Society for the Promotion of Science (JSPS) KAKENHI Grant Number 26410242. We thank UBE Scientific Analysis Laboratory, Inc., to measure XPS spectra of Pt-TiO_2 and perform boiling water extraction test for Cr-TiO_2.

References

[1] Photocatalytic Purification and Treatment of Water and Air, in: D.F. Ollis, H. Al-Ekabi (Eds.), Elsevier, Amsterdam, 1993.
[2] M.R. Hoffmann, S.T. Martin, W. Choi, D.W. Bahnemann, Chem. Rev. 95 (1995) 69–96.
[3] A. Fujishima, T.N. Rao, D.A. Tryk, J. Photochem. Photobiol. C: Photochem. Rev. 1 (2000) 1–21.
[4] U.I. Gaya, A.H. Abdullah, J. Photochem. Photobiol. C: Photochem. Rev. 9 (2008) 1–12.
[5] B. Ohtani, J. Photochem. Photobiol. C: Photochem. Rev. 11 (2010) 157–178.
[6] F. Fresco, R. Portela, S. Suarez, J.M. Coronado, J. Mater. Chem. A 2 (2014) 2863–2884.
[7] A. Fujishima, X. Zhang, D.A. Tryk, Surf. Sci. Rep. 63 (2008) 515–582.
[8] C.S. Enache, J. Schoonman, R.V. Krol, J. Electroceram. 13 (2004) 177–182.
[9] X.H. Wang, J.-G. Li, H. Kamiyama, Y. Moriyoshi, T. Ishigaki, J. Phys. Chem. B 110 (2006) 6804–6809.
[10] L.G. Devi, B.N. Murthy, S.G. Kumar, J. Mol. Catal. A: Chem. 308 (2009) 174–181.
[11] M. Nishikawa, Y. Mitani, Y. Nosaka, J. Phys. Chem. C 116 (2012) 14900–14907.
[12] B. Liu, H.M. Chen, C. Liu, S.C. Andrews, C. Hahn, P. Yang, J. Am. Chem. Soc. 135 (2013) 9995–9998.
[13] C. Andriamiadamanana, C.L. Robert, M.T. Sougrati, S. Casale, C. Davoisne, S. Patra, F. Sauvage, Inorg. Chem. 53 (2014) 10129–10139.
[14] M.G. Mota, A. Vojvodic, F.A. Pedersen, J.K. Norskov, J. Phys. Chem. C 117 (2013) 460–465.
[15] M. Anpo, M. Takeuchi, J. Catal. 216 (2003) 505–516.
[16] M. Takeuchi, M. Matsuoka, M. Anpo, Res. Chem. Intermed. 38 (2012) 1261–1277.
[17] Y. Shen, T.R.B. Foong, X. Hu, Appl. Catal. A: Gen. 409–410 (2011) 87–90.
[18] S. Kim, S.-J. Hwang, W. Choi, J. Phys. Chem. B 109 (2005) 24260–24267.
[19] J. Choi, H. Park, M.R. Hoffmann, J. Phys. Chem. C 114 (2010) 783–792.
[20] E. Wang, W. Yang, Y. Cao, J. Phys. Chem. C 113 (2009) 20912–20917.
[21] R. Zhang, A.A. Elzatahry, S.S. Al-Deyab, D. Zhao, Nano Today 7 (2012) 344–366.
[22] Q. Xu, M.A. Anderson, J. Mater. Res. 6 (1991) 1073–1081.
[23] S. Yamazaki, Y. Fujiwara, S. Yabuno, K. Adachi, K. Honda, Appl. Catal. B: Environ. 121–122 (2012) 148–153.
[24] W. Choi, A. Termin, M.R. Hoffmann, J. Phys. Chem. 98 (1994) 13669–13679.
[25] E. Hogfeldt, Stability Constants of Metal-ion Complexes, Part A: Inorganic Ligands, Pergamon Press, 1982.
[26] R.H. Byrne, W. Yao, Y.-R. Luo, B. Wang, Mar. Chem. 97 (2005) 34–48.
[27] V.S. Bryantsev, M.S. Diallo, W.A. Goddard, J. Phys. Chem. A 11 (2009) 9559–9567.
[28] W.A. Spieker, J. Liu, J.T. Miller, A.J. Kropf, J.R. Regalbuto, Appl. Catal. A: Gen. 232 (2002) 219–235.
[29] S. Kim, W. Choi, J. Phys. Chem. B 109 (2005) 5143–5149.
[30] J. Zhu, J. Ren, Y. Huo, Z. Bian, H. Li, J. Phys. Chem. C 111 (2007) 18965–18969.
[31] R. Santos, G.A. Faria, C. Giles, C.A.P. Leite, H.S. Barbosa, M.A.Z. Arruda, C. Longo, ACS Appl. Mater. Interfaces 4 (2012) 5555–5561.
[32] J. Zhu, F. Chen, J. Zhang, H. Chen, M. Anpo, J. Photochem. Photobiol. A: Chem. 180 (2006) 196–204.
[33] Q. Sun, Y. Xu, J. Phys. Chem. C 114 (2010) 18911–18918.
[34] K. Wilke, H.D. Breuer, J. Photochem. Photobiol. A: Chem. 121 (1999) 49–53.
[35] Practical surface analysis, in: D. Briggs, M.P. Seah (Eds.), Auger and X-ray Photoelectron Spectroscopy, vol. 1, 2nd ed., Wiley, West Sussex, England, 1990.
[36] J. Zhu, Z. Deng, F. Chen, J. Zhang, H. Chen, M. Anpo, J. Huang, L. Zhang, Appl. Catal. B: Environ. 62 (2006) 329–335.
[37] Y. Huang, H. Ma, S. Wang, M. Shen, R. Guo, X. Cao, M. Zhu, X. Shi, ACS Appl. Mater. Interfaces 4 (2012) 3054–3061.
[38] C.-J. Yang, Energy Policy 37 (2009) 1805–1808.
[39] H.-J. Choi, J.-S. Kim, M. Kang, Bull. Kor. Chem. Soc. 28 (2007) 581–588.
[40] Y. Li, W. Wang, X. Qiu, L. Song, H.M. Meyer, M.P. Paranthaman, G. Eres, Z. Zhang, B. Gu, Appl. Catal. B: Environ. 110 (2011) 148–153.
[41] H.-S. Chen, R.V. Kumar, RSC Adv. 2 (2012) 2294–2301.
[42] O. Kesmez, E. Burunkaya, N. Kiraz, H.E. Camurlu, M. Asilturk, E. Arpac, J. Non-Cryst. Solids 357 (2011) 3130–3135.
[43] M. Niederberger, Acc. Chem. Res. 40 (2007) 793–800.